FULL PAPER

Bis(oxazoline)titanium Complexes as Chiral Catalysts for Enantioselective Hydrosilylation of Ketones − A Combined Experimental and Theoretical Investigation

Marco Bandini,[a] Fernando Bernardi,[a] Andrea Bottoni,*[a] Pier Giorgio Cozzi,*[a] Gian Pietro Miscione,[a] and Achille Umani-Ronchi[a]

A combined experimental and theoretical investigation has been carried out on a new catalytic system, based on bis-(oxazoline) (BOX) complexes of titanium. These catalytic species are able to reduce aromatic ketones with good enantiomeric excesses and satisfactory yields. The experimental and the computational (DFT) evidence has provided useful information on the nature of the active catalytic species and on the mechanism of the reaction. The most likely reaction path involves a Ti^{IV} catalytic species. This result agrees with experimentally obtained evidence that seems to rule out the presence of Ti^{III} species. The analysis of the structure of the transition state corresponding to the reduction process (the addition of the hydride to the carbonyl system), provides an interesting insight on the enantioselectivity that characterizes this reaction.

(© Wiley-VCH Verlag GmbH & Co. KGaA, 69451 Weinheim, Germany, 2003)

Introduction

The development of chiral *ansa*-metallocene[1] catalysts for the stereospecific polymerization of propylene has encouraged chemists in industrial and academic laboratories to extend the use of the species to stereoselective organic synthesis. For instance, the chiral C_2 *ansa*-metallocenes [(EBTHI)MX$_2$] (M = Ti, Zr; X = OR, Cl, F; EBTHI = ethylenebis(tetrahydroindenyl)] introduced by Brintzinger can be used to mediate interesting asymmetric transformations.[2−3] In particular, chiral titanocene complexes [(EBTHI)TiX$_2$] are able to promote effectively the hydrosilylation of ketones and imines in high enantiomeric excess.[4] This synthetic approach has been included in industrial methods[5] and has been used to prepare biologically active products.[6] However, even though optically active [(EBTHI)TiF$_2$] complexes are now commercially available, their use remains quite expensive. The preparation of optically active chiral titanocenes is not in fact a trivial procedure, and great skill in organometallic synthesis and unusual facilities[7] are required.

Recently, the search for more effective and practical polymerization catalysts based on non-cyclopentadienyl frameworks has provided new and interesting ligands suitable for the coordination of early transition metals.[8−15] Among these, one interesting example is represented by the bis(oxazoline) (BOX) ligands (see Scheme 1).[16] Pioneering studies carried out by Pfaltz,[17] Evans,[18] Jørgensen,[19] and others[20] have shown that these chelating N∩N ligands are capable of coordinating many different metal atoms and are particularly suitable for asymmetric catalysis.
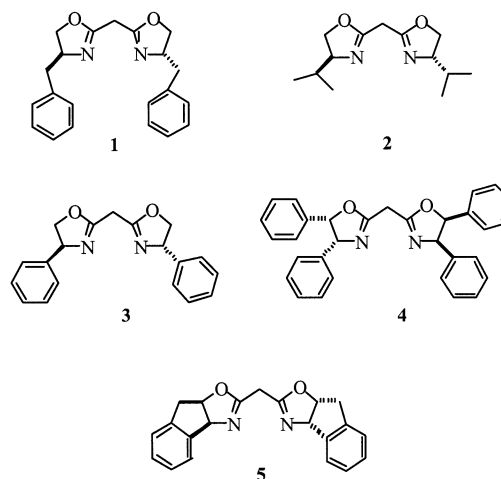
Scheme 1

The objective of the current study is to show that chiral EBTHI ligands can be replaced by commercially available or easily prepared chiral bis(oxazolines), avoiding the resolution process needed to obtain optically pure C_2 metallocenes. To this end the various BOX ligands shown in

Scheme 1 have been examined. In the new synthetic route that we propose, the *ansa*-bis(indenyl) anion is replaced by two bis(oxazolinate) anions obtained by deprotonation of the corresponding neutral ligands. To compare the performances of our (BOX)titanium complexes to those of *ansa*-titanocene complexes, we chose as a reference reaction the hydrosilylation of aromatic ketones in the presence of $(EtO)_3SiH$, since this reaction, mediated by chiral (ETBHI)-titanium complexes, has been widely investigated over the last decade.[21] In addition to the experimental study,[22] in order to obtain more detailed information on the mechanistic aspects of this reaction, we have also carried out a theoretical investigation at the DFT level.

Results and Discussion

Experimental Results

The BOX ligands **1**−**5** shown in Scheme 1 were used to prepare chiral organometallic complexes capable of replacing the $[(S,S)\text{-(ETBHI)TiF}_2]$ species. While BOX ligands **2**−**5** are commercially available, BOX ligand **1** was obtained by the general procedure described by Evans.[23] The metallation of the bis(oxazoline) species was performed under described conditions[24] (*n*BuLi, THF, −78 °C as summarized in Scheme 2, route A). Different titanium salts − $TiCl_4$, $TiCl_4(THF)_2$, $Ti(OiPr)_4$, $Ti(OiPr)_2Cl_2$, and TiF_4 − were employed with the BOX ligands **1**−**5** in the stoichiometric ratio 1:2. The addition of the titanium salt TiX_4 was carried out at 0 °C, giving a pale orange solution. This procedure provided various (BOX)titanium complexes that we used in the catalytic hydrosilylation of acetophenone. The reaction was found to be very slow with many silyl hydrides such as Et_3SiH, Cl_3SiH, Ph_3SiH, PMSH, and $(Me_3Si)_3SiH$. In contrast, though, we obtained much more interesting results from the more reactive $(EtO)_3SiH$[25] species, as re-

Table 1. Enantioselective hydrosilylation of acetophenone by use of various BOX ligands

Box	TiX_4 (mol %)	Yield (%)[a]	*ee* (%)[b]
1	$TiCl_4(THF)_2$ (4)	60	30 (*R*)
1[c]	$TiCl_4(THF)_2$ (3)	60	50 (*R*)
3	$TiCl_4(THF)_2$ (4)	20	23 (*R*)
1	$TiCl_2(OiPr)_2$ (15)	87	18 (*S*)
4	$TiCl_2(OiPr)_2$ (4)	85	51 (*S*)
5	$TiCl_2(OiPr)_2$ (3)	13	64 (*S*)
4	TiF_4 (5)	86	61 (*S*)
4[d]	TiF_4 (5)	28	72 (*S*)

[a] Isolated yields after chromatographic purification. [b] Percent enantiomeric excess was determined by chiral GC analysis (Megadex 5). [c] The reaction was carried out in the presence of molecular sieves (1 g). [d] The reaction was run in Et_2O.

ported in Table 1. From these data it is evident that the best results (yield and enantiomeric excess) were obtained through the use of TiF_4[26] and BOX ligand **4**.

' It is noteworthy that the (BOX)Ti complexes can be obtained by a simpler route in which Et_3N is used as a base (see Scheme 2, route B); the results obtained with different BOX ligands are collected in Table 2. We found that the titanium complexes prepared in this way were able to reduce acetophenone in satisfactory yields. However, in spite of the easier catalyst preparation, the enantiomeric excesses were significantly lower than those obtained from the reaction in which the catalyst was prepared with *n*BuLi. It is noteworthy that no activation steps[27] are necessary to perform the reduction of the acetophenone in either of our procedures.

Table 2. Enantioselective hydrosilylation of acetophenone by use of the (BOX)Ti complexes prepared with Et_3N

Box	TiF_4 (mol %)	Yield (%)[a]	*ee* (%)[b]
1	TiF_4 (10)	92	25 (*R*)
1	TiF_4 (5)	88	24 (*R*)
1[c]	TiF_4 (5)	84	24 (*R*)
3	TiF_4 (5)	84	18 (*R*)
4	TiF_4 (5)	75	51 (*S*)
4[d]	TiF_4 (5)	88	49 (*S*)

[a] Isolated yields after chromatographic purification. [b] Percent enantiomeric excess was determined by chiral GC analysis (Megadex 5). [c] Hünig base was used instead of Et_3N. [d] The reaction was carried out at −20 °C.
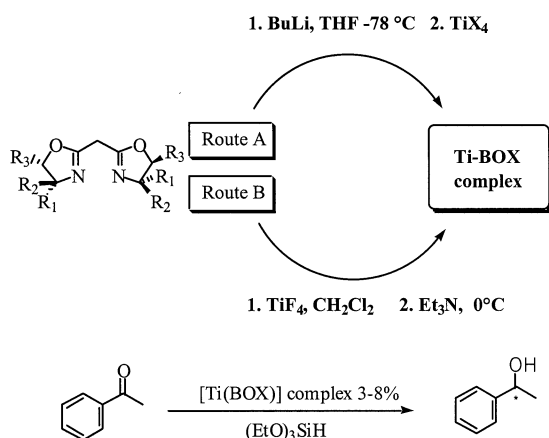
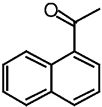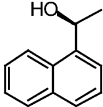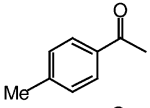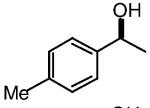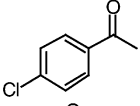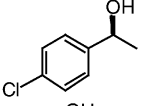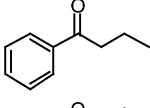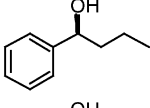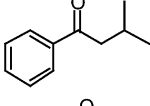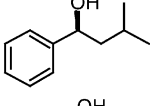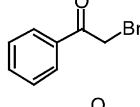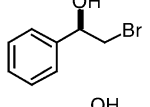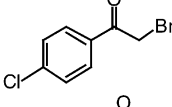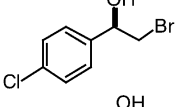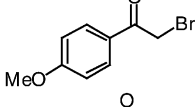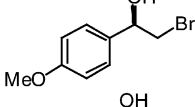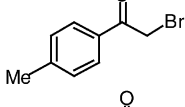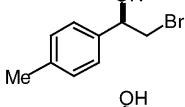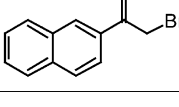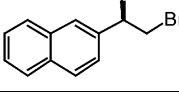To monitor the formation of the titanium complex we examined the NMR proton region in the δ = 6.0−5.4 ppm range for the chiral BOX ligand **4**. The free bis(oxazoline) has two protons, which appear as two doublets centered at δ = 5.98 and 5.65 ppm (AB system), respectively, with a coupling constant of $J = 9.0$ Hz. The addition of 1 equiv. of TiF_4 to 2 equiv. of BOX ligand **4** in CD_2Cl_2 caused the appearance of two broad signals at δ = 6.0−5.8 ppm and 5.8−5.65 ppm. This evidence suggested a fast exchange be-

1. BuLi, THF -78 °C 2. TiX₄

Route A

Route B

Ti-BOX complex

1. TiF₄, CH₂Cl₂ 2. Et₃N, 0°C

[Ti(BOX)] complex 3-8%

$(EtO)_3SiH$

Scheme 2

tween a titanium complex and the free BOX ligand **4**. Addition of 2 equiv. of Et$_3$N caused the appearance of two new doublets (δ = 5.89 and 5.41 ppm) and the vanishing of the two broad signals. The ratio between the two doublets of the free bis(oxazoline) ring and the two doublets of the newly formed species is 5.6:1. The ^{1}H NMR therefore suggested that the metallation results in the formation of only one species. Similar information was obtained from the ^{13}C NMR spectra (see Exp. Sect.). Furthermore, after metallation, the signal of the methine proton of the oxazoline bridge is shifted to low field: the new titanium species formed shows a singlet at δ = 4.69 ppm, while in the free BOX ligand the signal of the protons of the CH$_2$ bridge appear at δ = 3.88 ppm. These results are in agreement with those reported by Anwander[28] for the methine proton of the [Ln(BOX)$_2$] complexes (Ln = Y, La; δ = 4.61 and

4.52 ppm, respectively) and those obtained by Singh for the [Zn(BOX)Cl] complex.[29] This experimental evidence thus suggests that the (BOX)Ti complex formed in our case has similar structural features. The NMR spectra also indicate the formation of highly symmetric (BOX)titanium complexes.

Two important points should be stressed. Firstly, the addition of 1 equiv. of acetophenone into the NMR tube containing the complex does not affect the signals of the complex. This finding is in agreement with a coordinatively saturated (BOX)Ti complex. Secondly, the addition of 3 equiv. of triethoxysilane into the NMR tube again leaves the spectra unchanged and no evidence for the formation of paramagnetic species could be detected. This result makes the hypothesis of a mechanism involving Ti^{III} species unlikely.

Table 3. Enantioselective hydrosilylation of ketones[a]

Entry	Ketones	Alcohols	mol% cat.	Time (h)	ee (%)[b]	Yield (%)
1			4	80	51	60
2			5	80	43	50
3			5	48	34	81
4			5	48	75[d]	58
5			5	48	85	61
6			5	80	82	60
7			8	80	63	49
8			8	80	79	53
9			8	80	83	61
10			8	120	59[e]	64

[a] Reactions were run with the use of the (BOX)titanium catalyst, prepared in situ from **4** and TiF$_4$ in THF. [b] Percent enantiomeric excess was determined by chiral GC analysis (Megadex 5). [c] Isolated yield after purification. [d] The enantiomeric excess was evaluated on the corresponding silyl ether. [e] The enantiomeric excess was evaluated by HPLC (Chiralcel OD).
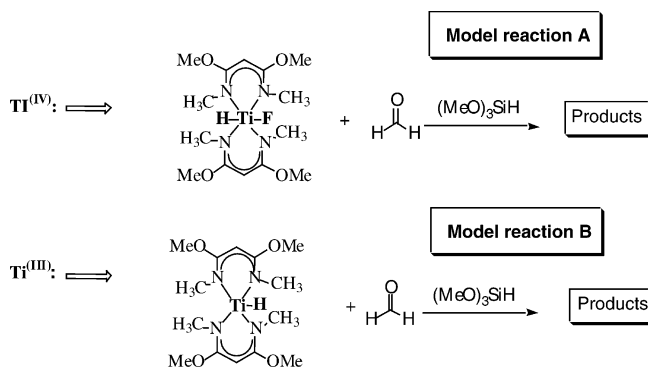
We now discuss the results obtained when the deprotonation of the BOX species was performed with *n*BuLi in [D$_8$]THF. Under these conditions, the recorded spectra for the titanium complex were similar to those previously discussed, while the ratio between the proton signals of the free BOX ligand and those of the new formed titanium species changed, becoming 1.5:1 in this case. The NMR analysis therefore indicates that the (BOX)titanium complexes obtained by the two different procedures correspond to the same species. All the various experimental results that we have discussed in detail, and also the data obtained in previous crystallographic studies[30] on stable titanium complexes, suggest that a plausible formula for the (BOX)Ti complex is [Ti(BOX)$_2$F$_2$].

The results obtained from the reduction of several aromatic ketones and substituted α-halo ketones with the best catalytic system represented in Scheme 2 (BOX ligand **4**, *n*BuLi in THF, and TiF$_4$) are collected in Table 3. These data show that satisfactory yields and good enantiomeric excesses were obtained.

As demonstrated by Buchwald,[4e] aromatic ketones are necessary in order to achieve high levels of enantioselectivity. To explain this observation, a model transition state in which a chiral metallocene titanium(III) hydride coordinates the ketone in a four-center (η^2) structure was proposed. Such a transition state does not seem suitable to explain the mechanism of the present reaction, based on (BOX)Ti complexes, where the presence of Ti^{III} species seems to be ruled out by the experimentally obtained evidence. Thus, to obtain more accurate information on the true nature of the active catalytic species present in solution (Ti^{III} or Ti^{IV} species) and to shed light on the mechanistic details of this reaction (the most probable reaction path, activation energies, reaction enthalpies, and free energies), we carried out a theoretical investigation at the DFT level. The results are discussed in the following section.

Computational Modeling

In our theoretical study we considered either a titanium(III) or a titanium(IV)[31] hydride complex as possible active species capable, in principle, of reducing the carbonyl substrate. These two species are schematically represented in the two model reactions A and B in Scheme 3. In each case, each of the two rings of the chelating BOX ligand, which is deprotonated in the CH$_2$ bridge position, was replaced by an OCH$_3$ group bonded to a carbon atom and a CH$_3$ group bonded to a nitrogen atom, while the ketone substrate was emulated by a formaldehyde molecule. The doublet (Ti^{III}) and singlet (Ti^{IV}) potential energy surfaces associated with these two model reactions are shown in Figure 1 and the critical points located along them are schematically represented in Figures 2 and 3 for reaction A, and Figures 4 and Figure 5 for reaction B. The values of the most relevant geometrical parameters and the energies relative to reactants are collected in the Figures. To check the reliability of this model system, we replaced the formaldehyde molecule with an acetone molecule and recomputed the structures of the critical points associated with the first steps of the two model reactions A and B. The results (geometrical parameters and energy values) obtained for this larger model system are reported in Figure 6. Plausible reactions that may produce Ti^{IV} or Ti^{III} complexes are illustrated in Scheme 4. For these processes we have assumed for L the simplified form of the BOX ligand chosen in our model system and we have replaced (EtO)$_3$SiH with (MeO)$_3$-SiH. The computed free energy values and the corresponding equilibrium constants are reported in Scheme 4.
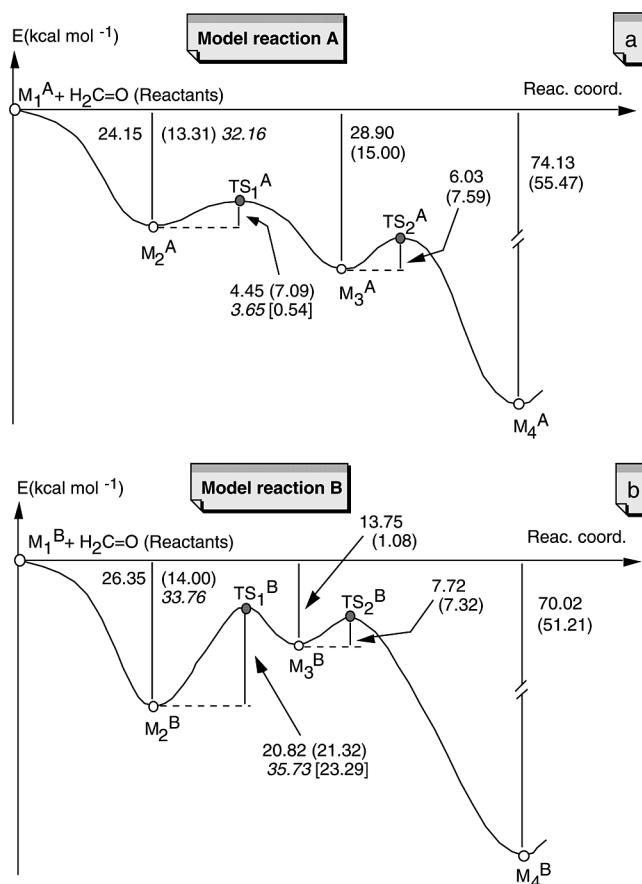
Figure 1. Energy profiles for model reaction A (Ti^{IV} catalytic species) and model reaction B (Ti^{III} catalytic species); free energy values are in parentheses; the MP2 values are in italics; the activation barriers obtained in the presence of solvent effects are reported in square brackets

Scheme 3
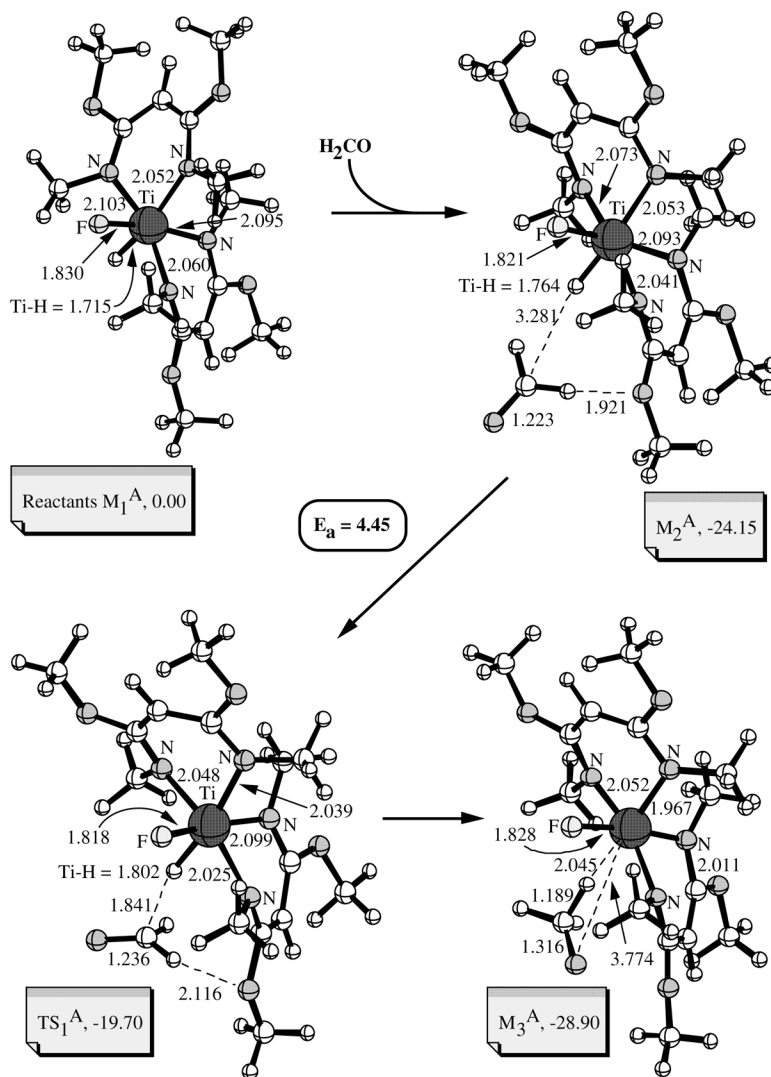
Figure 2. Schematic representation of the structures of the four critical points M_1^A, M_2^A, TS_1^A, and M_3^A; the energy and the free energy (in parentheses) values [kcal·mol^{-1}] relative to reactants (M_1^A + H_2CO) and the most relevant geometrical parameters [Å] are reported; the absolute total energy and free energy values of reactants are -2121.0583 and -2120.6691 Hartree, respectively

Figure 3. Schematic representations of the structures of the two critical points TS_2^A and M_4^A; the energy and the free energy (in parentheses) values [kcal·mol^{-1}] relative to reactants (M_1^A + H_2CO) and the most relevant geometrical parameters [Å] are given

Figure 4. Schematic representations of the structures of the four critical points M_1^B, M_2^B, TS_1^B, and M_3^B; the energy and the free energy (in parentheses) values [kcal·mol^{-1}] relative to reactants (M_1^B + H_2CO) and the most relevant geometrical parameters [Å] are given; the absolute total energy and free energy values of reactants are -2021.6734 and -2022.2904 Hartree, respectively

Model Reaction A: The [(L)₂TiFH] Catalyst

The energy profile for model reaction A is shown in Figure 1, part a. The reaction is a three-step process, and is highly exothermic ($\Delta E = -74.13$ kcal·mol^{-1}). Six critical points were located along the energy profile: M_1^A, M_2^A, TS_1^A, and M_3^A (Figure 2), together with TS_2^A and M_4^A (Figure 3). In M_1^A, which represents the active form of the catalyst, the coordination of the metal atom is octahedral with two Ti−N bonds in axial positions (2.060 and 2.103 Å, respectively). The first intermediate M_2^A forms from M_1^A and an isolated formaldehyde molecule without any barrier (M_2^A is 24.15 kcal·mol^{-1} lower in energy than the reactants) and corresponds to a long-range complex in which the formaldehyde molecule weakly interacts with the catalyst. The distance between the hydrogen atom bonded to the titanium atom and the formaldehyde carbon atom is still 3.281 Å, but a hydrogen bond forms between one formaldehyde hydrogen atom and the oxygen atom of one

OCH_3 group (the H···O distance is 1.921 Å). This interaction seems to be responsible for the significant stabilization observed for M_2^A, although we should point out that this stabilization is probably overestimated because of the small basis set on the oxygen atom. This hydrogen bond has the effect of placing the substrate in the best position for the subsequent hydride transfer (transition state TS_1^A). The role played by this H bond in determining the spatial orientation of the formaldehyde is equally evident in TS_1^A, in which the H···O distance is only slightly longer (2.116 Å) than in M_2^A. It is important to point out that the orienting effect of the hydrogen bond is not a shortcoming of the model system used here, since the involved oxygen atom is present in the same position in the real system. The reported geometrical parameters indicate that the transition state TS_1^A has a strongly reactant-like character, since the breaking Ti−H bond is still 1.802 Å (1.715 and 1.764 Å in M_1^A and M_2^A, respectively) and the newly forming C−H
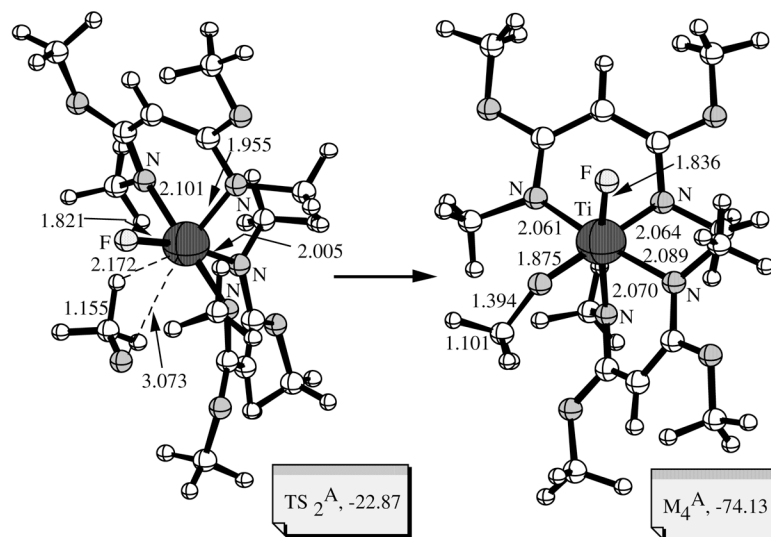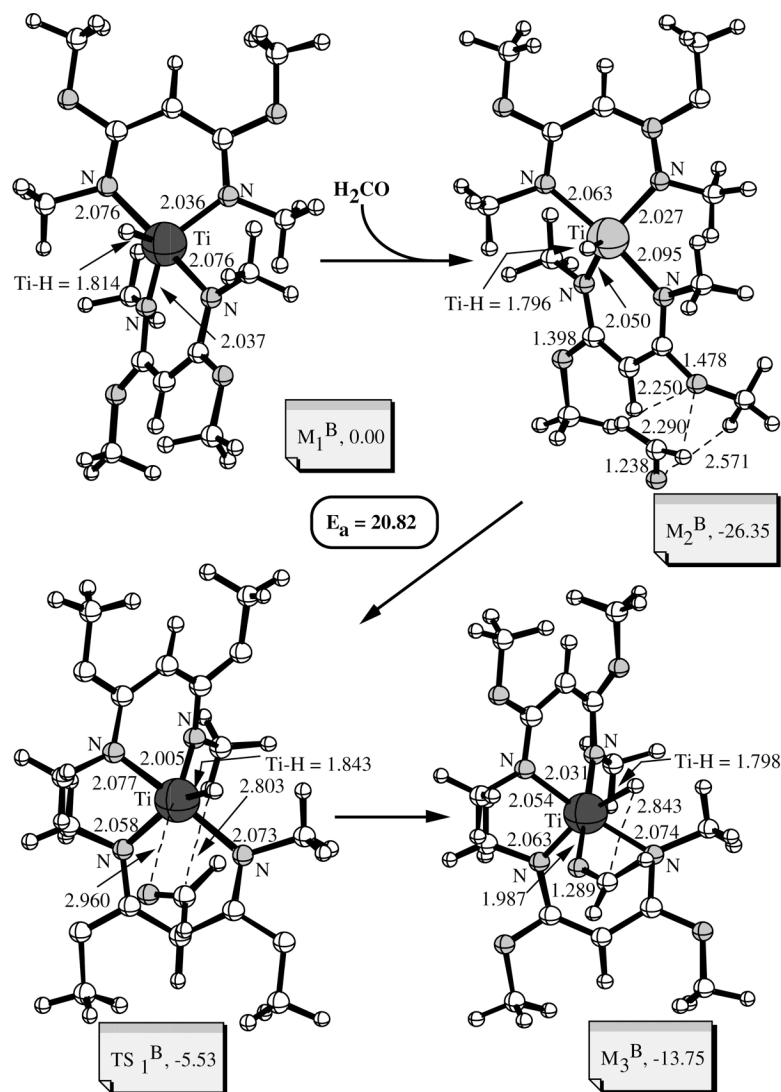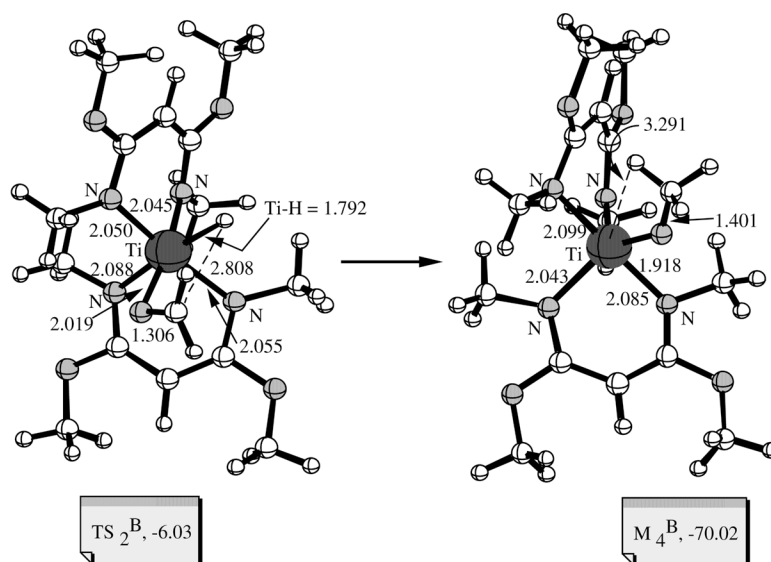
Figure 5. Schematic representations of the structures of the two critical points TS_2^B and M_4^B; the energy and the free energy (in parentheses) values [kcal·mol^{-1}] relative to reactants ($M_1^B + H_2CO$) and the most relevant geometrical parameters [Å] are given
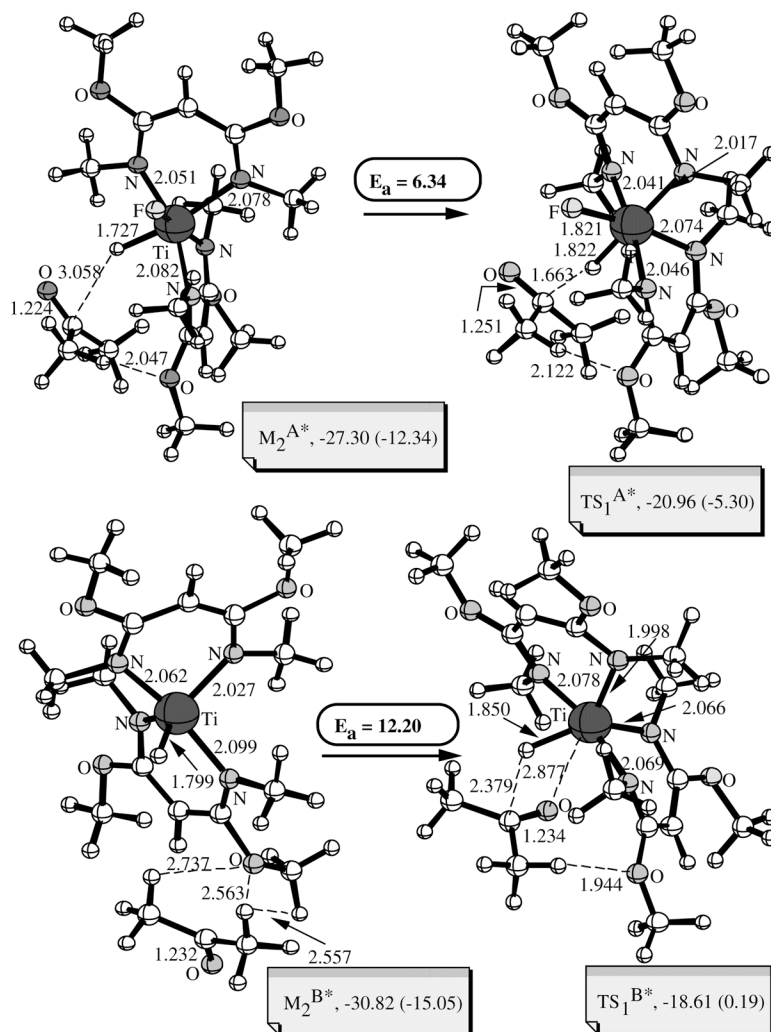
Figure 6. Schematic representations of the structures of the four critical points M_1^{A*}, TS_1^{A*}, M_1^{B*}, and TS_1^{B*}; the energy and the free energy (in parentheses) values [kcal·mol^{-1}] relative to reactants and the most relevant geometrical parameters [Å] are given; total and free energies of reactants: -2199.7168 (E) and -2199.2759 (G) Hartree (reaction A); -2100.3319 (E) and -2100.8972 (G) Hartree (reaction B)

1 $[(L)_2Ti^{(IV)}F_2] + (MeO)_3SiH \rightleftharpoons [(L)_2Ti^{(IV)}\mathbf{H}(F)] + (MeO)_3SiF$

$\Delta G = 9.38 \text{ kcal mol}^{-1}$, $K_{eq} = 1.24 \times 10^{-7}$

2 $[(L)_2Ti^{(IV)}H(F)] \rightleftharpoons [(L)_2Ti^{(III)}F] + 1/2 \text{ } H_2$

$\Delta G = -24.55 \text{ kcal mol}^{-1}$, $K_{eq} = 1.18 \times 10^{18}$

3 $[(L)_2Ti^{(III)}F] + (MeO)_3SiH \rightleftharpoons [(L)_2Ti^{(III)}\mathbf{H}] + (MeO)_3SiF$

$\Delta G = 17.10 \text{ kcal mol}^{-1}$, $K_{eq} = 2.59 \times 10^{-13}$
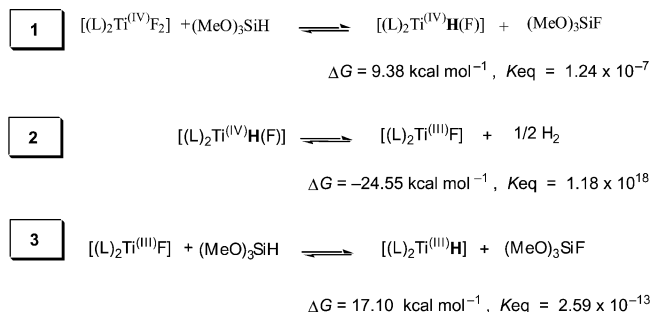
L = model BOX ligand of Scheme 3

Scheme 4

bond is only 1.841 Å. A slight lengthening of the carbonyl bond (1.236 Å), which is losing its double-bond character, is also observed. TS_1^A leads to a second intermediate M_3^A, in which the new C–H bond is almost complete (1.189 Å) and the negative oxygen atom interacts slightly with the positive titanium atom, the Ti–O distance now being 3.774 Å. The transformation $M_2^A \rightarrow M_3^A$ requires the overcoming of an energy barrier of 4.45 kcal·mol^{-1}, and M_3^A is 4.75 kcal·mol^{-1} lower in energy than M_2^A. An additional transition state TS_2^A leads from M_3^A to the final product M_4^A. In TS_2^A the H_3CO group rotates in such a way as to position the negative oxygen atom closer to the metal atom. Here the Ti–O distance becomes 3.073 Å and the hydrogen atom still weakly interacts with the metal atom, the Ti–H distance being 2.172 Å. A barrier of 6.03 kcal·mol^{-1} characterizes this transformation. In the final product, M_4^A, only the oxygen atom of the H_3CO fragment is coordinated to the titanium atom. The Ti–O bond is now 1.874 Å and the carbonyl group has definitely lost its double-bond character (the C–O bond is 1.394 Å).

In addition to the total energy values, we also computed the free energy values, which are reported for the various critical points in parentheses in the diagram of Figure 1, part a. The free energy profile is similar to that of the total energy previously discussed. The reaction is still highly exothermic (55.47 kcal·mol^{-1}) and the two free energy barriers that must be overcome to obtain the product remain quite small (7.09 and 7.59 kcal·mol^{-1}, respectively). Thus, both sets of values (total energies and free energies) indicate that carbonyl reduction promoted by the Ti^{IV} catalytic species is a quite easy reaction. However, it is important to stress that, while the activation energies and the activation free energies are very similar, more significant variations are observed when we compare the relative energies and relative free energies of M_2^A, M_3^A, and M_4^A. For instance the energy and free energy (relative to the asymptotic limit) of M_2^A are 24.15 and 13.31 kcal·mol^{-1}, respectively. This remarkable change is certainly due to the anomalous contributions of low frequencies appearing in the presence of weakly interacting fragments such as in $M_1^A + H_2C=O$ and M_2^A.

B. Model Reaction B: The [(L)$_2$TiH] Catalyst

The energy profile for model reaction B (see Figure 1, b) is very similar to that discussed in the previous section. The

reaction, which is exothermic by -70.02 kcal·mol^{-1}, is again a three-step process characterized by six critical points along the energy profile: M_1^B, M_2^B, TS_1^B, and M_3^B (Figure 4), together with TS_2^B and M_4^B (Figure 5). The active complex M_1^B corresponds to a distorted trigonal bipyramid in which two Ti–N bonds (2.076 Å) are situated in axial positions. As previously observed along the reaction profile A, a preliminary complex M_2^B, 26.35 kcal·mol^{-1} lower in energy than the reactants, forms from M_1^B and an isolated formaldehyde molecule. This transformation again occurs without any barrier. In the M_2^B species the formaldehyde molecule forms two hydrogen bonds with the oxygen atom of one OCH_3 group. These two hydrogen bonds are fairly strong, as suggested by the two H···O distances (2.025 and 2.290 Å, respectively) and the energy lowering of the system. From M_2^B it is possible to reach a new intermediate M_3^B through the transition state TS_1^B. In TS_1^B, which has a product-like character, the formaldehyde molecule moves away from the H_3CO group to coordinate the metal atom. Here, the H_2CO molecule interacts significantly with the titanium atom (the Ti–O distance is 2.960 Å), while the distance between the titanium-bonded hydrogen atom and the carbonyl carbon atom is still large (2.803 Å). In the intermediate M_3^B, the Ti–O and C···H distances become 1.987 and 2.843 Å, respectively. Thus, in this complex, which corresponds to a square bipyramid with the formaldehyde molecule in equatorial position, the Ti–O bond is almost complete. M_3^B is higher in energy than M_2^B by 12.60 kcal·mol^{-1} and the barrier required for the transformation $M_2^B \rightarrow M_3^B$ (the rate-determining step of the process) is 20.82 kcal·mol^{-1}. A computation of the intrinsic reaction coordinate (IRC)[32] was carried out, starting from TS_1^B in both reactant and product directions, to demonstrate how the three critical points M_2^B, TS_1^B, and M_3^B are connected on the reaction surface. It is interesting to note the different natures of the corresponding critical points located for model reaction A (i.e., M_2^A, TS_1^A, and M_3^A, in comparison to those of M_2^B, TS_1^B, and M_3^B). In the former case we showed that the hydrogen bond, which immediately forms in M_2^A, has the effect of positioning the substrate molecule in the right position for the hydride attack. In the latter case, in contrast, two hydrogen bonds must be broken to move the formaldehyde molecule close enough to the Ti–H bond and to make the reduction process possible. This could explain the larger activation barrier found for TS_1^B. A second transition state (TS_2^B), with an activation barrier of 7.72 kcal·mol^{-1}, affords the final product M_4^B. In TS_2^B the formaldehyde molecule rotates around the C–O bond to position the molecular plane orthogonal to the approaching direction of the hydride ion. This transition state has a strongly reactant-like character and the distance between the hydrogen atom and the formaldehyde carbonyl atom is still large (2.808 Å). In addition, no weakening of the Ti–H bond (1.792 Å) is observed. The final product M_4^B is a trigonal bipyramid in which the H_3CO fragment, obtained after reduction, is situated in an equatorial position and two nitrogen atoms are in axial positions. The final O–Ti distance is 1.918 Å, while the C–O

carbonyl bond has become 1.401 Å, as one can expect for a single C−O σ bond.

The free energy values (reported in parentheses in Figure 1, b) provide information similar to that obtained from the total energy curve. The reaction is still highly exothermic (-51.21 kcal·mol^{-1}) and, even if the intermediate M_3^B is significant higher in energy (it becomes almost degenerate to reactants), the two energy barriers associated with TS_1^B and TS_2^B do not change significantly, being 21.32 and 7.32 kcal·mol^{-1} respectively.

The Solvent Effect

The activation energies of the first reaction step for both model systems ($M_2^A \rightarrow TS_2^A$ and $M_2^B \rightarrow TS_2^B$ transformations) were recomputed with allowance for solvent effects. The emulated solvent in the COSMO computations is tetrahydrofuran (dielectric constant ε = 7.58), the solvent used in the real experiment. In the presence of the solvent the activation barriers for the two model reactions A and B (values in square brackets in Figure 1) become 0.54 and 23.29 kcal·mol^{-1}, respectively. Thus, even when the environment solvent effect is taken into account, the reaction channel involving Ti^{IV} species is still highly favored.

MP2 Computations

The total energies of the first three critical points along the two reaction profiles ($M_1^A + H_2CO$, M_2^A, TS_1^A and $M_1^B + H_2CO$, M_2^B, and TS_1^B) were recomputed at the MP2 level. The results are reported in italics in Figure 1. For both reaction pathways the formation of the first intermediate (M_2^A and M_2^B) again provides a strong stabilization of the system: 32.16 and 33.76 kcal·mol^{-1}, respectively. Furthermore, the activation barriers for the first step ($M_2^A \rightarrow TS_1^A$ and $M_2^B \rightarrow TS_1^B$) are 3.65 and 35.73 kcal·mol^{-1}. The MP2 method thus provides the same mechanistic scenario as obtained at the DFT level: the reaction pathway corresponding to model reaction A (Ti^{IV} species) is again much more likely than that found for model reaction B (Ti^{III} species). These results also indicate that the large stabilization found for the first intermediate complex is not a shortcoming of the computational method.

The Model System Involving Acetone

The structures of the critical points M_2^A and TS_1^A (model reaction A) and M_2^B and TS_1^B (model reaction B) were recomputed after the formaldehyde molecule had been replaced with an acetone molecule. The four new computed structures are denoted as M_2^{A*}, TS_1^{A*}, M_2^{B*}, and TS_1^{B*} (see Figure 6).

The intermediate M_2^{A*} is 27.30 kcal·mol^{-1} lower in energy than the reactants (isolated acetone + M_1^A). This value is fairly close to that for M_2^A (24.15 kcal·mol^{-1}). The structures of M_2^A and M_2^{A*} are quite similar. M_2^{A*} again corresponds to a long-range complex in which the acetone molecule interacts weakly with the titanium catalyst. The key interaction, which moves the substrate to a suitable position for the subsequent hydride transfer, is the hydrogen

bond between a methyl hydrogen atom of the ketone and the oxygen atom of one methoxy group. The H···O distance is 2.047 Å (it was 1.921 Å in M_2^A). Similarly, the distance between the titanium-bonded hydrogen atom and the acetone carbon atom (3.058 Å) does not differ significantly from the value found in the case of formaldehyde (3.281 Å). TS_1^{A*} also has a structure similar to that of TS_1^A. As pointed out in the case of formaldehyde, the H bond, characterized here by an H···O distance of 2.122 Å, is important for maintaining the spatial orientation of the substrate. The structural parameters computed for TS_1^{A*} indicate a more strongly product-like character than TS_1^A, since the breaking Ti−H bond and the newly forming C−H bond are now 1.822 and 1.663 Å, respectively. However, this stronger product-like character is associated with an increase in the activation energy, which becomes 6.34 kcal·mol^{-1} (4.45 kcal·mol^{-1} with formaldehyde). It is reasonable to ascribe this larger barrier to an increase in the steric hindrance associated with the acetone methyl groups.

As observed for reaction A, the results obtained for M_2^{B*} and TS_1^{B*} are also very close to those described for M_2^B and TS_1^B, respectively. The preliminary complex M_2^{B*} is 30.82 kcal·mol^{-1} lower in energy than that of the reactants (M_1^B and isolated acetone) and its formation does not require any energy barrier. The reduction in energy with respect to the reactants is again caused by the formation of two hydrogen bonds between the methyl hydrogen atoms and the oxygen atom of one H_3CO group. The H···O distances in this case are 2.737 and 2.563 Å. In TS_1^{B*} the acetone molecule behaves similarly to that of the formaldehyde molecule in TS_1^B and thus moves closer to the titanium atom. The Ti−O distance becomes 1.850 Å and that between the titanium-bonded hydrogen atom and the carbonyl carbon atom 2.379 Å. To approach the metal atom, the acetone molecule must break one hydrogen bond as observed in TS_1^B. The breaking of this bond determines the entity of the activation barrier for the transformation $M_2^{B*} \rightarrow TS_1^{B*}$. Even if this barrier decreases with respect to the simpler model based on formaldehyde (it now becomes 12.20 kcal·mol^{-1}), it remains much larger than that found for reaction A. The pathway involving Ti^{IV} species is thus also favored over that based on Ti^{III} complexes in the presence of acetone as substrate. A similar conclusion can be reached from the free energy values reported in parentheses in Figure 6; the free activation barriers for the two model reactions A and B are, in fact, 7.04 and 15.28 kcal·mol^{-1}, respectively. These results suggest that the simpler model system based on formaldehyde emulates the reaction satisfactorily.

Discussion

Comparison of the two reaction profiles (A and B) suggests that the reaction involving the Ti^{IV} species should be faster than that promoted by the Ti^{III} complex. Although the two reactions are characterized by similar exothermicity values, the activation barrier of the rate-determining step in

the Ti^{III} case (20.82 kcal·mol^{-1}), is much higher than the two barriers found along the Ti^{IV} reaction pathway (4.45 and 6.03 kcal·mol^{-1}, respectively). This evidence, and the data obtained for the reactions reported in Scheme 4, which are assumed to produce the two possible active species, may help in the proposal of a reasonable mechanistic scenario for the whole catalytic process.

The free energy values and the corresponding equilibrium constants reported in Scheme 4 indicate that the equilibrium corresponding to reaction (1) is moved to the left, so only a few [L]$_2$Ti^{IV}(F)H molecules are available to catalyze the reaction. This result is in agreement with the experimentally obtained NMR spectroscopic data: as previously pointed out, we were not able to identify any new species generated by the reaction between the silyl hydride and the (BOX)titanium complex from the NMR spectra.

Similar computational evidence was found for the Ti^{III}-based catalyst. The formation of this catalytic species requires two consecutive reactions: reaction (2), which gives the [L]$_2$TI^{III}F complex, and reaction (3), in which the fluorine atom is replaced by the hydrogen atom to give the active complex [L]$_2$Ti^{III}H. Even if reaction (2) is thermodynamically favored, however, reaction (3) is highly endothermic with a very small equilibrium constant, so the formation of the [L]$_2$Ti^{III}H catalyst is highly disfavored. The low concentrations of both catalytic species in the reaction medium should favor the reduction pathway characterized by the lowest activation barriers: that involving the [L]$_2$Ti^{IV}(F)H complex. Since this is an easy process (low activation barriers and high exothermicity), it is reasonable to believe that the Ti^{IV} active species is immediately involved in the reduction as soon as it is formed and that reaction (1) is forced to produce additional [L]$_2$Ti^{IV}(F)H complexes to restore the equilibrium constant. This hypothesis points to the Ti^{IV} complex as the catalytically active species truly involved in the reduction, in agreement with the experimentally obtained data, from which we had no evidence for the existence of Ti^{III} species.

The mechanism that we propose on the basis of our combined experimentally determined and computational results corresponds to a catalytic cycle such as that schematically represented in Scheme 5. In this cycle the catalytic species [L]$_2$Ti^{IV}(F)H (L = deprotonated BOX ligand) forms from [L]$_2$Ti^{IV}F$_2$ and (EtO)$_3$SiH (reaction 1 in Scheme 4). The reduction of the carbonyl compound (R$_1$R$_2$C=O) affords the [L]$_2$Ti^{IV}OCHR$_1$R$_2$ complex, as found in the investigation of the reaction surface. This complex reacts with the (EtO)$_3$-SiH species to provide the silyl alcohol (EtO)$_3$SiOCHR$_1$R$_2$ (final product) and the [L]$_2$Ti^{IV}(F)H complex, which restores the catalytic species.

As pointed out in the previous discussion, the transition state TS$_1^A$ describes the reduction process (i.e., the addition of the hydride ion to the carbonyl system). It is interesting to analyze the structure of TS$_1^A$, since it can explain the experimentally observed stereoinduction in this reaction. When, instead of the formaldehyde or acetone model substrate, the acetophenone molecule approaches the active complex M$_2^A$, it is much easier for the substrate molecule
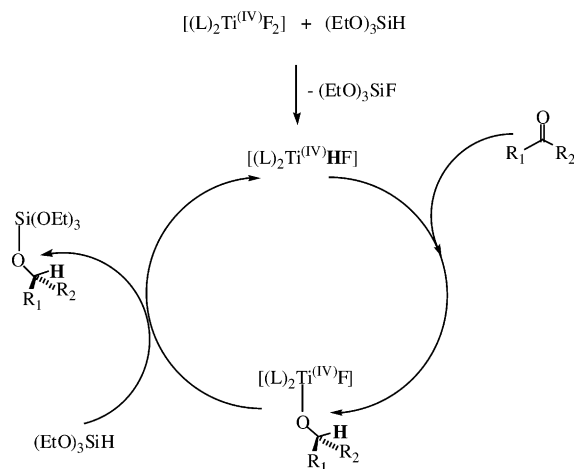
Scheme 5

to accommodate the more cumbersome phenyl group in the less crowded molecular region, as indicated in Figure 7. This particular arrangement should reduce the steric hindrance between the titanium catalyst and the benzene ring. At the same time it allows the formation of a stabilizing interaction (hydrogen bond) between the oxygen atom of one BOX ligand and one hydrogen atom of the carbonyl substrate.[33] In our model system (in particular that based on acetone) the formation of this hydrogen bond is evident. It involves one methyl hydrogen atom of acetone and one oxygen atom of the BOX ligand (as indicated in Figures 6 and 7). It is worth pointing out that, even in the case of the simple model system used here to emulate the (BOX)titanium complex, the expected absolute configuration of the alcohol product obtained from acetophenone is (S) in agreement with the experimentally obtained observation.
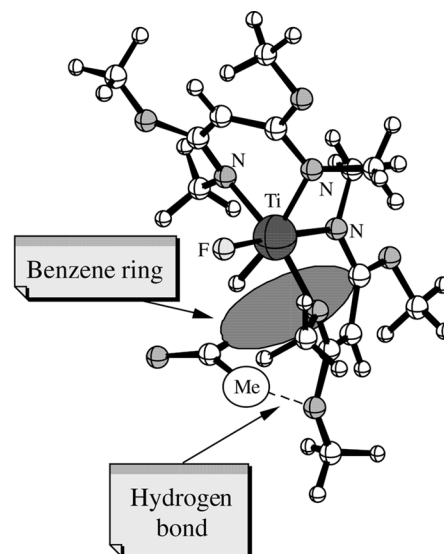
Figure 7. Schematic representation of the arrangement of the acetophenone substrate in the TS$_1^A$ transition state (model reaction **A**)

Conclusions

We have carried out a combined experimental and theoretical investigation of a new catalytic system based on bis-(oxazoline) (BOX) complexes of titanium, which is able to reduce aromatic ketones with good enantiomeric excesses and satisfactory yields. We have demonstrated that these BOX complexes can effectively replace the more expensive chiral C_2 metallocene species.

The experimentally acquired evidence and the computational results, obtained at the DFT level, have provided useful information on the nature of the active catalytic species and on the mechanism of the reaction. The DFT computations demonstrated the existence of two possible reaction paths: one originating from a Ti^{IV} catalytic species (model reaction A) and the other from a Ti^{III} complex (model reaction B). Although both reaction channels are thermodynamically favored (they are highly exothermic), the former is characterized by much lower activation energies than the latter. This result points to the $(BOX)Ti^{IV}$ complex as the true active catalyst involved in the reaction and agrees with the experimentally acquired evidence (NMR spectra), which seems to rule out the presence of Ti^{III} species. The analysis of the structure of the transition state corresponding to the reduction process [i.e., the addition of the hydride ion to the carbonyl system (TS_1^A)], also provides an interesting insight into the enantioselectivity that characterizes this reaction.

The computation of the solvent effects for the two transformations $M_2^A \rightarrow TS_1^A$ and $M_2^B \rightarrow TS_1^B$ does not change the mechanistic picture, and the pathway corresponding to model reaction A remains highly favored. Similar conclusions were obtained from MP2 computations on the DFT-optimized structures.

Experimental Section

General Procedure for the Asymmetric Hydrosilylation of Ketones by Use of [Ti(BOX)$_2$F$_2$] Complexes Prepared with *n*BuLi: The desired BOX ligand (**1**−**5**, 0.16 mmol) was dissolved in degassed THF (2 mL) in a flame-dried flask, which was cooled to −78 °C. A solution of *n*BuLi in hexane (1.6 M, 0.08 mmol) was added, the reaction mixture was stirred for 10 min, and the pale yellow solution was then warmed to 0 °C. Solid TiF$_4$ (9.8 mg, 0.08 mmol) was added, and the reaction mixture was vigorously stirred. The solution turned orange and was stirred at room temperature for 1 h. The ketones (1 mmol) and triethoxysilane (***WARNING:*** The vapors can cause blindness!) (2 mmol) were added, and the reaction mixture was stirred for 48−80 h. The reaction mixture was diluted with Et$_2$O, and NaOH (2 M) was then carefully added. The mixture was stirred at room temperature for 30 min, and the organic phase was separated. The aqueous phase was extracted with Et$_2$O. The combined organic phases were dried with sodium sulfate and then concentrated under reduced pressure to give an oil, which was purified by flash chromatography (cyclohexane/Et$_2$O, 8:2 to 9:1).

NMR Studies: [D$_8$]THF was vacuum-transferred into a flame-dried flask. Bis(oxazoline) **4** (70 mg, 0.15 mmol) was added, and the resulting solution was cooled to −78 °C. *n*BuLi (2.5 M, 60 µL, 0.15 mmol) was added, the pale yellow solution was stirred at

−78 °C for 10 min, and then warmed to 0 °C. TiF$_4$ (9.3 mg, 0.075 mmol), stored under nitrogen in sealed vials, was then added, and the resulting mixture was rapidly stirred at room temperature until the formation of an orange solution. The resulting solution was transferred by syringe into a flame-dried NMR tube, stored in a dried Schlenk flask. The tube was closed with a stopcock and stored under nitrogen until the spectra had been recorded. Diagnostic signals for the titanium complex: ^{1}H NMR ([D$_8$]THF, 200 MHz): δ = 5.87 (d, J = 8.4 Hz, 2 H), 5.41 (d, J = 8.4 Hz, 2 H), 4.59 (s, 1 H) ppm. ^{13}C NMR ([D$_8$]THF, 50 MHz): δ = 30.48, 58.61, 69.43, 85.34, 137.48, 139.93, 168.40 ppm.

Computational Details: All the DFT computations were performed with the Gaussian 98[34] series of program, with use of the non-local hybrid Becke's three-parameter exchange functional denoted as B3LYP.[35] It has been shown elsewhere that this functional is able to provide reliable results for organotitanium complexes. These results agree very well both with experimentally determined data and with the results obtained at higher levels of theory, such as the MP2 and CASPT2 approaches.[36] In all cases the geometries of the various critical points on the reaction surface were fully optimized by the gradient method available in Gaussian 98. A heterogeneous basis set was used. The DZVP basis set,[37] which is a Local Spin Density (LSD)-optimized basis set of double-zeta quality in the valence shell plus polarization functions, was used for the titanium atom, the hydrogen atom involved in the reduction process, and the atoms of the formaldehyde molecule. The 3-21G basis set[38] was employed for the atoms directly bonded to the metal atom, while the minimal STO-3G basis[39] was used to describe all the remaining atoms. A computation of the harmonic vibration frequencies was carried out to determine the natures of the various critical points. To check the reliability of the computational level used here (basis set and B3LYP functional), we compared the computed geometrical parameters to the experimentally derived X-ray parameters. Since the X-ray structures for the titanium complexes investigated in this work have not been determined, we chose as a reference compound a similar Ti^{III} complex (represented in Figure 8), the structure of which is available in the literature.[40] Inspection of the results reported in Figure 8 shows that the computed structure agrees fairly well with the experimentally determined one. This suggests that our computational approach is acceptable for investigation of this class of metal complexes. In addition to total energy
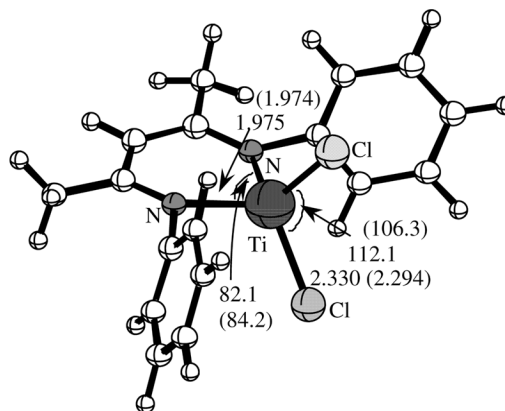

Figure 8. Schematic representation of the titanium complex reported in ref.[40], with the values of the most important geometrical parameters obtained at the B3LYP level; the corresponding experimentally determined values are reported in parentheses (bond lengths are in Å and angles in °)

values, free energy values were also considered for the various critical points. Free energies were obtained from frequency calculations within the RRHO approximation. This approximation can provide only a rough estimate of free energy trends. This is especially true in situations such as those examined here, in which, in the presence of weakly interacting fragments, low frequencies and thus anomalous contributions to free energy can be expected. For rough evaluation of the effect of the solvent environment, we carried out single-point computations on the gas-phase optimized structures for some critical points, by use of the continuous model approach COSMO[41] as implemented in the Turbomole package.[42]

[1] [1a] H. H. Brintzinger, D. Fisher, R. Mülaupt, B. Rieger, R. M. Waymouth, *Angew. Chem. Int. Ed. Engl.* **1995**, *34*, 1143−1170. [1b] A. H. Hoveyda, J. P. Morken, in *Metallocene* (Eds.: A. Togni, R. L. Halterman), Wiley-VCH, Weinheim, **1998**, p. 625, and references therein.

[2] A. H. Hoveyda, J. Morken, *Angew. Chem. Int. Ed. Engl.* **1996**, *35*, 1262−1284.

[3] [3a] S. Collins, Y. Hong, B. A. Kuntz, *J. Org. Chem.* **1989**, *54*, 4154−4158. [3b] T. Takahashi, D. Y. Kodankov, N. Suzuki, *Organometallics* **1994**, *13*, 3411−3412. [3c] E. Negishi, M. D. Jensen, D. Y. Kodankov, S. M. Wang, *J. Am. Chem. Soc.* **1994**, *116*, 8404−8405.

[4] [4a] M. B. Carter, B. Schiøtt, A. Gutièrrez, S. L. Buchwald, *J. Am. Chem. Soc.* **1994**, *116*, 11667−11670. [4b] X. Verdaguer, U. E. W. Lange, M. T. Reding, S. L. Buchwald, *J. Am. Chem. Soc.* **1996**, *118*, 6784−6785. [4c] X. Verdaguer, U. E. Lange, S. L. Buchwald, *Angew. Chem. Int. Ed.* **1998**, *37*, 1103−1107. [4d] M. C. Hansen, S. L. Buchwald, *Org. Lett.* **2000**, *2*, 713−715. [4e] J. Yun, S. L. Buchwald, *J. Am. Chem. Soc.* **1999**, *121*, 5640−5644.

[5] The titanocene methodology was patented by: S. L. Buchwald, R. B. Grossman, A. Gutièrrez, US 5227538 assigned to M. I. T., **1993**.

[6] J. Yun, S. L. Buchwald, *J. Org. Chem.* **2000**, *65*, 767−774.

[7] See for example: [7a] G. M. Diamond, R. F. Jordan, J. L. Petersen, *J. Am. Chem. Soc.* **1996**, *118*, 8024−8033. [7b] Q. Yang, M. D. Jensen, *Synlett* **1996**, 147−148.

[8] [8a] R. Uhrhamer, D. G. Black, T. G. Gardner, J. D. Olsen, R. F. Jordan, *J. Am. Chem. Soc.* **1993**, *115*, 8493−8494. [8b] E. B. Tjaden, D. C. Swenson, R. F. Jordan, J. L. Petersen, *Organometallics* **1995**, *14*, 371−386. [8c] A. J. Blake, J. M. McInnes, P. Mounford, G. I. Nikonov, D. Swallow, D. J. Watkin, *J. Chem. Soc., Dalton Trans.* **1999**, 379−392.

[9] [9a] R. R. Schrock, R. Bauman, S. M. Reid, J. T. Goodman, R. Stumpf, W. M. Davis, *Organometallics* **1999**, *18*, 3649−3670. [9b] T. I. Goutntchev, T. Don Tilley, *Organometallics* **1999**, *18*, 5661−5667. [9c] A. D. Horton, J. de With, *Organometallics* **1997**, *16*, 5424−5436. [9d] N. A. H. Male, M. Thortnon-Pett, M. Bochman, *J. Chem. Soc., Dalton Trans.* **1997**, 2487−2494. [9e] R. Baumann, W. M. Davis, R. R. Schrock, *J. Am. Chem. Soc.* **1997**, *119*, 3830−3831. [9f] J. D. Scollard, D. H. McConville, S. J. Rettig, *Organometallics* **1997**, *16*, 1810−1812. [9g] J. D. Scollard, D. H. McConville, *J. Am. Chem. Soc.* **1996**, *118*, 1008−1009. [9h] M. Schubart, L. O'Dwyer, L. H. Gade, W. S. Li, M. McPartlin, *Inorg. Chem.* **1994**, *33*, 3893−3898.

[10] H. Brand, J. Arnold, *J. Am. Chem. Soc.* **1992**, *114*, 2266−2267. H. Brand, J. Arnold, *Organometallics* **1993**, *12*, 3655−3665.

[11] L. Giannini, C. Caselli, E. Solari, C. Floriani, A. Chiesi-Villa, C. Rizzoli, M. Re, A. Sgamellotti, *J. Am. Chem. Soc.* **1997**, *119*, 9709−9719.

[12] A. Caselli, L. Giannini, E. Solari, C. Floriani, N. Re, A. Chiesi-Villa, C. Rizzoli, *Organometallics* **1997**, *16*, 5457−5469.

[13] D. P. Steinhuebel, S. J Lippard, *Organometallics* **1999**, *18*, 109−111.

[14] [14a] G. D. Whitener, J. Hagadorn, J. Arnold, *J. Chem. Soc., Dalton Trans.* **1999**, 1249−1255. [14b] J. R. Hagadorn, J. Arnold, *Organometallics* **1998**, *17*, 1355−1368. [14c] V. Volkis, M. Shmulinson, C. Averbuj, A. Lisovskii, F. T. Edelmann, M. Eisen, *Organometallics* **1998**, *17*, 3155−3157.

[15] [15a] G. Rodriguez, G. C. Bazan, *J. Am. Chem. Soc.* **1995**, *117*, 10155−10156. [15b] R. Kempe, P. Arndt, *Inorg. Chem.* **1996**, *35*, 2644−2649. [15c] B. Qian, W. J. Scanlon IV, M. R. Smith III, D. H. Motry, *Organometallics* **1999**, *18*, 1693−1698. [15d] A. J. Ashe, III, X. Fang, J. W. Kampf, *Organometallics* **1999**, *18*, 1363−1365. [15e] S. J. Brown, X. Gao, D. G. Harrison, L. Koch, R. E. v. H. Spence, G. P. A. Yap, *Organometallics* **1998**, *17*, 5445−5447. [15f] G. G. Lavoie, R. G. Bergman, *Angew. Chem. Int. Ed. Engl.* **1997**, *36*, 2450−2452. [15g] S. K. Bertilsson, L. Tedenborg, D. A. Alonso, P. G. Anderson, *Organometallics* **1999**, *18*, 1281−1286.

[16] For a recent review see: P. Braunstein, F. Naud, *Angew. Chem. Int. Engl.* **2001**, *40*, 680−699, and ref. therein.

[17] A. Pfaltz, *Acc. Chem. Res.* **1993**, *26*, 239−345.

[18] D. A. Evans, J. A. Murry, P. V. von Matt, R. D. Norcross, S. J. Miller, *Angew. Chem. Int. Ed. Engl.* **1995**, *34*, 798−800. [18a] D. A. Evans, S. J. Miller, T. Lectka, P. von Matt, *J. Am. Chem. Soc.* **1999**, *121*, 7559−7573.

[19] [19a] J. Thorhauge, M. Johannsen, K. A. Jørgensen, *Angew. Chem. Int. Ed.* **1998**, *37*, 2404−2406. [19b] S. Yao, M. Johannsen, H. Audran, R. G. Hazell, K. A. Jørgensen, *J. Am. Chem. Soc.* **1998**, *120*, 8599−8605.

[20] A. K. Ghosh, P. Mathivanan, J. Cappiello, *Tetrahedron: Asymmetry* **1998**, *9*, 1−45, and references therein.

[21] [21a] H. Imma, M. Mori, T. Nakai, *Synlett* **1996**, 1229−1230. [21b] R. L. Halterman, T. M. Ramsey, Z. Chen, *J. Org. Chem.* **1994**, *59*, 2642−2644.

[22] Part of these results has been already presented: M. Bandini, P. G. Cozzi, L. Negro, A. Umani-Ronchi, *Chem. Commun.* **1999**, 39−40.

[23] D. A. Evans, G. S. Peterson, J. S. Johnson, D. M. Barnes, K. R. Campos, K. A. Woerpel, *J. Org. Chem.* **1999**, *64*, 678−678.

[24] M. Nakamura, A. Hirai, M. Sogi, E. Nakamura, *J. Am. Chem. Soc.* **1998**, *120*, 5846−5847.

[25] The reactivity of silanes has been shown to decrease in the order $(EtO)_3SiH > (EtO)_2Si(Me)H > PMHS > Ph_2SiH_2$. However, the reagent has potential hazards, see: K. Barr, S. C. Berk, S. L. Buchwald, *J. Org. Chem.* **1994**, *59*, 4323−4326. As the $(EtO)_3SiH$ is reported to be a toxic reagent, other hydride source were examined. We discovered that catecholborane can be used as hydride source with BOX ligands, but that lower enantiomeric excess was determined in all cases.

[26] The reaction between the deprotonated BOX ligand and TiF_4 can be performed by direct addition of TiF_4, or the TiF_4 can be added dissolved in CH_3CN.

[27] The active catalyst, starting from the pre-catalyst [(*S,S*)-(EB-THI)TiF$_2$], was prepared by Buchwald by addition of phenylsilane, pyrrolidine and MeOH sequentially, and heating at 60 °C until the color of the solution changed from yellow to green. No explanation for this procedure and no investigations on the species prepared in such a way has been presented. The previous procedure suggests that the activation step depends on the way *n*BuLi is added to the reaction mixture (see the experimental procedure described in ref.[4a])

[28] H. W. Görlitzer, M. Spiegler, R. Anwander, *J. Chem. Soc., Dalton Trans.* **1999**, 4287−4288.

[29] In a series of [Zn(BOX)X] complexes the signal of the CH_2 protons, which appears at δ ≈ 3.3 ppm in the free bis(oxazolines), were found to be shifted to δ ≈ 4.7 ppm (CH form). See: R. P. Singh, *Bull. Soc. Chim. Fr.* **1997**, *134*, 765−768.

[30] P. G. Cozzi, C. Floriani, A. Chiesi-Villa, C. Rizzoli, *Inorg. Chem.* **1995**, *34*, 2921−2930.

[31] For the structure of a titanium(III) atom, surrounded by non-Cp ligands, see: J. B. Love, H. S. C. Clark, F. G. N. Cloke, J. C. Green, P. B. Hitchcock, *J. Am. Chem. Soc.* **1999**, *121*, 6843−6849.

[32] C. Gonzalez, H. B. Schlegel, *J. Chem. Phys.* **1989**, *90*, 2154−2161.

[33] Recent evidence for this kind of hydrogen bond has recently been provided in theoretical and experimental investigations: [33a] N. Bernardi, A. Bottoni, S. Casolari, E. Tagliavini, *J. Org. Chem.* **2000**, *65*, 4783. [33b] E. J. Corey, T. W. Lee, *Chem. Commun.* **2001**, 1321−1329.

[34] M. J. Frisch, G. W. Trucks, H. B. Schlegel, G. E. Scuseria, M. A. Robb, J. R. Cheeseman, V. G. Zakrzewski, J. A. Jr. Montgomery, R. E. Stratmann, J. C. Burant, S. Dapprich, J. M. Millam, A. D. Daniels, K. N. Kudin, M. C. Strain, O. Farkas, J. Tomasi, V. Barone, M. Cossi, R. Cammi, B. Mennucci, C. Pomelli, C. Adamo, S. Clifford, J. Ochterski, G. A. Petersson, P. Y. Ayala, Q. Cui, K. Morokuma, D. K. Malick, A. D. Rabuck, K. Raghavachari, J. B. Foresman, J. Cioslowski, J. V. Ortiz, B. B. Stefanov, G. Liu, A. Liashenko, P. Piskorz, I. Komaromi, R. Gomperts, R. L. Martin, D. J. Fox, T. Keith, M. A. Al-Laham, C. Y. Peng, A. Nanayakkara, C. Gonzalez, M. Challacombe, P. M. W. Gill, B. Johnson, W. Chen, M. W. Wong, J. L. Andres, M. Head-Gordon, E. S. Replogle, J. A Pople, *Gaussian 98*, revision A.6, Gaussian, Inc., Pittsburgh, PA, **1998**.

[35] [35a] A. D. Becke, *J. Chem. Phys.* **1993**, *98*, 5648−5652. [35b] C. Lee, W. Yang, R. G. Parr, *Phys. Rev.* **1988**, *B37*, 785.

[36] F. Bernardi, A. Bottoni, G. P. Miscione, *Organometallics* **1998**, *17*, 16.

[37] N. Godbout, D. R. Salahub, J. Andzelm, E. Wimmer, *Can. J. Chem.* **1992**, *70*, 560−571. UniChem. DGauss, Version 2.3.1, Cray Research, Inc., Seattle, **1994**.

[38] J. S. Binkley, J. A. Pople, W. J. Hehre, *J. Am. Chem. Soc.* **1980**, *102*, 939−947. W. J. Pietro, M. M. Francl, W. J. Hehre, D. J. Defrees, J. A. Pople, J. S. Binkey, *J. Am. Chem. Soc.* **1982**, *104*, 5039−5048.

[39] W. J. Hehre, R. F. Stewart, J. A. Pople, *J. Chem. Phys.* **1969**, *51*, 2657. J. B. Collins, P. v. R. Schleyer, J. S. Binkley, J. A Pople, *J. Chem. Phys.* **1976**, *64*, 5142.

[40] P. H. M. Budzelaar, A. B. van Oort, A. G. Orpen, *Eur. J. Inorg. Chem.* **1998**, 1485−1494.

[41] A. Klamnt, *J. Phys. Chem.* **1995**, *99*, 2224. A. Klamnt, *J. Phys. Chem.* **1996**, *100*, 3349.

[42] *Turbomol*, version 5.6, Institut für Physikalische Chemie und Elektrochemie Lehrstuhl für Theoretische Chemie, Universität Karlsruhe, Kaiserstr. 12, 76128 Karlsruhe, Germany, **2002**.